Journal of Archaeological Science 39 (2012) 1871–1882

Contents lists available at SciVerse ScienceDirect

Journal of Archaeological Science

journal homepage: http://www.elsevier.com/locate/jas

# Archaeomagnetic data from four Roman sites in Tunisia

Boutheina Fouzai [a], Lluís Casas [b,*], Néjia Laridhi Ouazaa [a], Aureli Álvarez [b]

[a] Université de Tunis El Manar, Unité de Recherche: Pétrologie Cristalline et Sédimentaire, Faculté des Sciences, Département de Géologie, Campus Universitaire, 2092 Manar II, Tunisia
[b] Universitat Autònoma de Barcelona, Facultat de Ciències, Departament de Geologia, Edifici C, Campus UAB, 08193 Bellaterra, Catalonia, Spain

ARTICLE INFO

*Article history:*
Received 2 August 2011
Received in revised form
23 January 2012
Accepted 26 January 2012

*Keywords:*
Archeomagnetism
Dating
Geomagnetic field modeling
Tunisia
Archaeodirections
Archaeointensities

ABSTRACT

Archaeomagnetic analyses on bricks and slag fragments from kilns have been undertaken. The initial aim of the paper was to constraint the age of four Roman sites in Tunisia (Neapolis, Pheradi Majus, Leptiminus and Sullecthum) using either archaeodirections or archaeointensities. However, the archaeomagnetic models appeared to be only proficient using directions. It has been established that the Neapolis' studied kiln was probably active until the early 6th century AD, whereas the kilns investigated in Pheradi Majus were probably active until the middle 5th century AD. Measured archaeointensities point to higher values than those predicted by the models during the whole range of possible ages for the studied sites.



## 1. Introduction

Dating tools are currently fundamental to characterize archaeological sites and artifacts. Besides typological-based chronologies the progress of science has produced different archaeometric dating tools, among them archaeomagnetic dating. This technique is based on the reconstruction of the variations of the geomagnetic field during the past using the thermoremanent magnetisation (TRM) stored in certain archaeological structures and artifacts. The use of archaeomagnetic dating tools has become more and more attractive as some well-established secular variation curves (SVC) have been available for reference sites (e.g. Le Goff et al., 2002; Gómez-Paccard et al., 2006; Zananiri et al., 2007). To produce these curves magnetic information from material dated accurately and independently (i.e. dated from non-magnetic methods) has to be extracted. These curves relate the variations of the geomagnetic field (its direction and/or intensity) to time. Besides SVC, data compilations from different countries and eras have also been used to build-up regional (Pavón-Carrasco et al., 2009) or global models of the secular variation (Korte et al., 2009). Reading the magnetic information from archaeological sites is of interest both for well-dated and poor-dated sites. The first contribute to create or update SVC and geomagnetic models, the latter permit to make hypothesis on the age of the site.

At present the majority of archaeomagnetic publications deal with sites located in countries with good archaeomagnetic analytical facilities (Casas et al., 2008). In order to improve our knowledge about the geomagnetic field history, archaeomagnetic studies should be extended to other countries (Lengyel et al., 2011).

Tunisia is fortunate to possess a rich historical past which has been the origin of several investigations both of historical and scientific order. Tunisian archaeological excavations tend to focus on the pottery (production centers, trading routes, manufacture techniques, etc), therefore the presence of kilns is highlighted in published records. We had the opportunity to apply archaeomagnetic techniques on some pottery kilns dating back from Roman times in several Tunisian locations along the eastern coast of Tunisia, namely from north to south: Neapolis (Nabeul), Pheradi Majus (Sidi Khélifa), Leptiminus (Lamta) and Sullecthum (Salakta) (see Fig. 1).

## 2. Historical and archaeological background of the studied sites

### 2.1. Neapolis

Neapolis is one of the first African cities to be reported by old historians, Thucydides refers to it as a Carthaginian trading city in

* Corresponding author. Tel.: +34 935868365; fax: +34 935811263.
*E-mail address:* Lluis.Casas@uab.es (L. Casas).

0305-4403/$ – see front matter © 2012 Elsevier Ltd. All rights reserved.
doi:10.1016/j.jas.2012.01.030

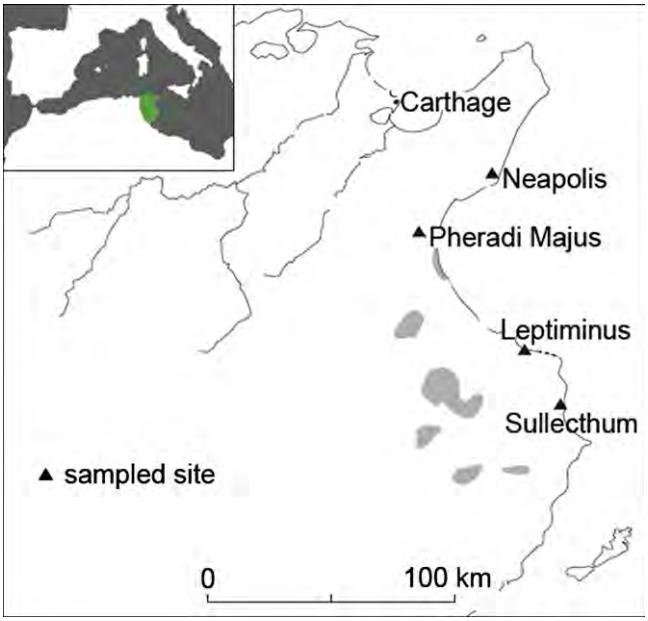


**Fig. 1.** Location of the sampled archaeological sites in Tunisia.

his texts written in the 5th century BC. The city was conquered by the Romans during the 3rd Punic war and later converted into a Roman colony. The Greek name has evoluted to Nabeul, which is the name of the modern village. It lies about 65 km south-east from Tunis, on the south coast near to the Cap Bon peninsula. The archaeological site is 2 km south-west from the centre of Nabeul. Archaeological excavations started during the sixties (20th century) and are mainly restricted to a fish salting factory and a Roman villa (named *Nympharum domus* according to a mosaic from its peristyle, (Darmon, 1980)). The salting factory was build during the 1st century AD and was active until the 3rd or 4th century (Sternberg, 2000). Several coins were found under the mosaics of the Roman villa and allowed to state that its *terminus post quem* is the second decade of the 4th century (Darmon, 1980) and its occupation continued until the 6th or 7th century (Sternberg, 2000). Pottery fragments recovered from the excavation of the villa are from the 7th century (late ARS, of Hayes 105 type). In the last fifteen years, several kilns and tombs have appeared within the destruction layer of street that passed north to the villa as well as in the south-west part of the villa. Their fillings include again ceramic fragments from the 7th century or later (Sternberg, 2000).

### 2.2. Pheradi Majus

Pheradi Majus is located in the vicinity of Sidi Khélifa (100 km south from Tunis, in the Enfida region), major excavations of the site started during the sixties of 20th century though to date only a small portion of the site area has been excavated. Exposed remains include a centre containing a triumphal arch, a forum and a nymphaeum. To the east, on a hill, there are the remains of sacred temples. To the north there are the thermae, also excavated. An artisan's district (Ben Moussa, 2007) spreads out to the west and the south-west along with an amphitheatre (both not yet excavated). This district has been severely damaged due to agricultural activities but excessive presence of fragments of late ARS (*terra sigillata*) ceramics is a clear indication of their existence and hints of kilns also appear on the surface, in 1997 and 1999 several prospections were made and a kiln was excavated (Ben Moussa, 2007).

The site occupation possibly dates back to the 3rd century BC though the most intense activity on the site developed during Roman times. Dating of the main excavated structures has been attempted from typological features of ceramics (Ben Moussa, 2007). The forum area would have been active from preimperial times (Punic) but it recorded maximum activity during the 1st century AD, *terminus ante quem* for this area would be the second half of 2nd century. The thermae would have been abandoned at the end of 4th century AD. Finally, concerning the artisan's neighborhood, prospections indicate activity during late antiquity (Ben Moussa, 2007), including activity during the Vandal times (Leone, 2007), thus kilns fillings contain basically ARS (*terra sigillata*) ceramics dated from 4th to 5th centuries.

### 2.3. Leptiminus

Leptiminus was an important Roman port city, its remains are located on the west of the modern town of Lamta, in the Sahel region, it lies 35 km south from Sousse (ancient Hadrumetum), 12 km south from Monastir (ancient Ruspina). The existence of Leptiminus or Leptis Minus, to distinguish it from Leptis Magna (present Libya), was long attested by literary evidence and archaeological finds (Stirling et al., 2000). The site is open agricultural land, gently undulating, crossed by wadis, featuring a considerable number of olive trees and surrounded by modern towns (Lamta, Bou Hadjar and Ksibet el Mediouni). Since 1990, an excavation project (Leptiminus Archaeological Project, LAP) has conducted field surveys and selected excavations (Stirling et al., 2001). Among these, in the so-called 'site 290', on a ridge at the eastern edge of the ancient town, a complex of five two-storeyed circular kilns was brought to light in 1995–1998 (Stirling et al., 2001). LAP project has allowed a deeper knowledge of Leptiminus and several studies has been published about the site (Sherriff et al., 2002a and 2002b; Keenleyside et al., 2009).

Nearby finds to site 290 indicate prehistoric (site 250) and Punic (site 285) activity (Stirling et al., 2001). However, finds at kilns from site 290 and scattered wasters indicate that they were used during Roman times to produce ARS ceramics, coarse wares and specially amphorae (Africana 1 and 2 Series) (Mattingly et al., 2000; Stirling et al., 2001). The kilns were active from the late 1st century AD to the 3rd century AD (Stirling et al., 2000) and their productions have been identified among the cargoes of Roman shipwrecks (Gibbins, 2001) and within Roman rubbish dumps (Whittaker, 2000).

### 2.4. Sullecthum

Sullecthum was also a Roman port located, presently, under the modern coastal village of Salakta, about 50 km south from Monastir, also in the Sahel region. The presence of an important amphorae production centre nearby Salakta was already known in the 19th century (Nacef, 2007), main production include Africana 1, 2A, 2D and Keay 25 amphorae types (Gibbins, 2001; Nacef, 2007). Like Leptiminus, stamped amphorae produced in the site have been identified in Roman shipwrecks (Gibbins, 2001) and rubbish dumps (Whittaker, 2000).

The site is largely integrated into the modern urban fabric. Four sites containing coastal ceramic productions have been reported (Peacock et al., 1989). They group in what would had been two concentrated peri-urban industrial zones (on one hand the sites labeled as El Hri I and II and on the other hand the sites

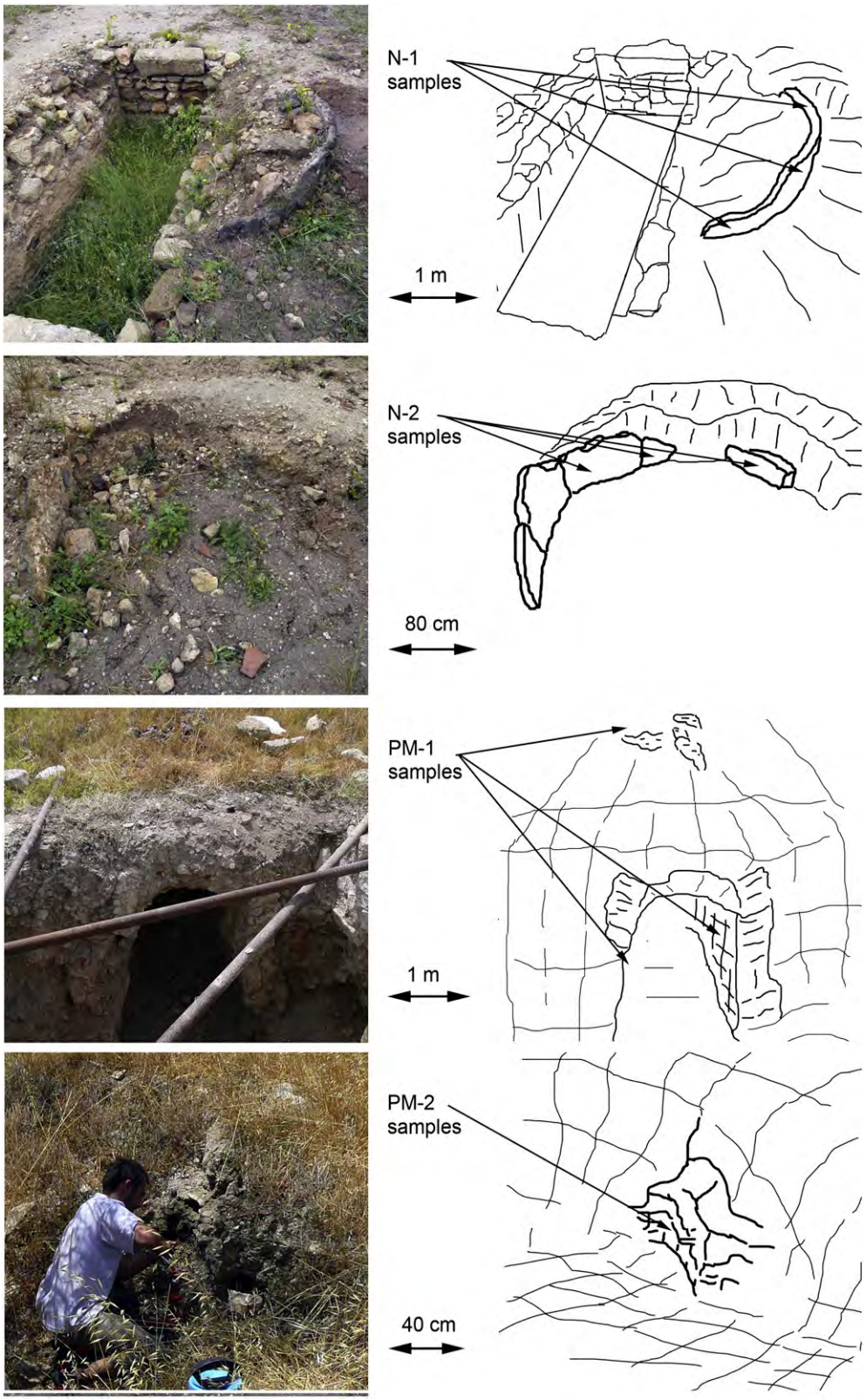


**Fig. 2.** Photographs and sketches of the structures from which samples were retrieved in-situ. From top to bottom: Pottery kiln N-1, Lime kiln N-2, both from Neapolis; Pottery kilns PM-1 and PM-2, both from Pheradi Majus.

labeled as Salakta and Catacombs) (Gibbins, 2001). Using the typology of amphorae and pottery Nacef, (2007) estimated that the activity in these workshops started towards the end of the 2nd century and continued until the 4th century. Later amphorae production in the area moved inland (Gibbins, 2001) and according to Nacef (2007) was not active before the 6th century.

## 3. Materials sampled

Two types of archaeomagnetic techniques have been applied: i) Archaeodirection analysis was applied for sites where the kilns were directly accessible. For those sites a number of cylindrical samples (~2.5 cm diameter) were collected using a portable electrical drill with a water-cooled diamond bit, following the standard palaeomagnetic sampling procedure. The in-situ azimuth and dip of the cores were measured using a compass coupled to a core orienting fixture. The samples were taken from parts of the kilns with clear evidence of repeated exposure to intense heat during firing, when possible structures covered by melting products (slag) were sampled. The samples taken were not very long in order to collect parts that were closer to the heat source; in general each sample produced a single specimen. ii) Archaeointensity analysis was mainly applied for the sites where the kilns were not accessible; sampling consisted in the collection of slag fragments around the kiln area. These fragments were cut into standard cylindrical specimens in the laboratory.

In Neapolis, two kilns located in the south-west part of the Nympharum domus were sampled. Both kilns are not fully excavated but its upper part was accessible to retrieve oriented samples (Fig. 2). One of the kilns (labeled here as N-1) produced pottery and is cut by a late inhumation structure, the other kiln (N-2) produced lime. Both are presumably from the 6th or 7th century and its stored archaeomagnetic directions were measured.

Two kilns from the artisan's district in Pheradi Majus were sampled (Fig. 2). One of them is a kiln that was partially excavated in the works of 1997 and 1999 labeled as kiln 2 in (Ben Moussa, 2007) but here labeled as PM-1. Oriented samples were retrieved from the excavated firebox and the kiln vaults accessible from the top. The other one possibly corresponds to kiln 1 in (Ben Moussa, 2007) and here is labeled as PM-02. Its structure is much more damaged but oriented samples were retrieved from its walls. Besides that, several slag fragments (PM-SS) were collected in the area to produce archaeointensities, including disoriented bricks from both kilns.

Sampling at the kiln complex in Leptiminus (site 290 in (Stirling et al., 2000)) was unfortunately inaccessible because it was reburied to preserve it. We were restricted to the collection of slag around the positions of kilns (L-SS), which are believed to have been active during the 2nd and 3rd centuries.

The so-called Catacombs site, in Sullecthum, is about 1 km south from the modern village of Salakta. There are clear indications that this site hosts a ceramic production center but it is also a Punic necropolis. Its kilns have never been excavated but scattered fragments of amphorae, pottery and slag cover the area. Sampling was restricted to collection of slag (S-SS). Pottery fragments recovered from the fillings of the catacombs entrance form small mounds on the site mixing with ceramics from kiln dumps. Two different dumps have been identified (Nacef, 2008) and from their contents it has been established that the kilns from the area were active from the late 1st century AD to the early 3rd century AD (Nacef, 2008).

To sum up, 87 samples were obtained from four archaeological sites from Tunisia with presumed ages ranging from the 1st century to the 7th century AD. Table 1 summarizes the details of all sites and samples.

**Table 1**
Coordinates of the sampled sites with indication of their presumed ages according to archaeological evidence, sample labels and number of collected samples.

| Site | Latitude (°N) | Longitude (°E) | Presumed age | Sampled structure | Label | *N* |
|---|---|---|---|---|---|---|
| Neapolis | 36.44 | 10.72 | 6th–7th AD | Kiln | N-1 | 8 |
| | | | | Kiln | N-2 | 9 |
| Pheradi Majus | 36.25 | 10.40 | 4th–5th AD | Kiln | PM-1 | 18 |
| | | | | Kiln | PM-2 | 5 |
| | | | | Scattered slag | PM-SS | 12 |
| Leptiminus | 35.67 | 10.87 | 2nd–3rd AD | Scattered slag | L-SS | 23 |
| Catacombs (Sullecthum) | 35.38 | 11.03 | 1st–3rd AD | Scattered slag | S-SS | 12 |

*N*, number of collected samples.

## 4. Experimental methods and data analyses

All laboratory works were done at the Paleomagnetic Laboratory of Barcelona (SCT UB-CSIC). The results were compared with model predictions using a Matlab dating tool developed by Pavón-Carrasco et al. (2011). Two models were used: the regional model SCHA.DIF.3K (Pavón-Carrasco et al., 2009) and the global model CALS3K.3 (Korte et al., 2009). The SCHA.DIF.3K model was obtained by least-sums of absolute deviation inversion of paleomagnetic data using spherical cap harmonics (SCHA) and provides geomagnetic field vector values over the European continent, Northern Africa and western Asia from 1000 BC to 1900 AD. The CALS3K.3 model was generated using a compilation of archaeomagnetic and lake sediments data covering the past 3000 years. Although CALS3K.3 is a global model, the distribution of data is strongly biased towards the northern hemisphere, and Europe in particular, thus the model provides reasonable field values especially for these regions. The use of archaeomagnetic field models avoids the need for relocation of archaeomagnetic data to a central location, which is a procedure that involves an inherent error (Casas and Incoronato, 2007).

### 4.1. Archaeodirection analyses

Measurements consisted of stepwise demagnetization of the natural remanent magnetization (NRM) and measurement of it at each step. Thermal demagnetization was performed in a Schönstedt TSD-1 demagnetizer and magnetization measurements on a 2G Enterprises superconducting rock magnetometer. Results were represented as Zijderveld diagrams (Zijderveld, 1967). Characteristic remanent magnetization (ChRM) directions were calculated by principal component analysis (Kirschvink, 1980) and usually involved only the remanence values measured after demagnetizing at 350–400 °C and higher temperatures. Specimens with a maximum angular deviation (MAD) higher than 5 (Hervé et al., 2011) or with ChRM not pointing to the origin in the Zijderveld diagrams were removed from the calculation of a mean direction. The specimen-sample hierarchy was observed to compute mean directions for each structure. This computation was achieved by using Fisher (1953) statistics, concentration parameter $k$ and confidence factor $\alpha_{95}$ were also obtained.

### 4.2. Archaeointensity analyses

The Coe variant method of a Thellier-type experiment was applied (Coe, 1967), the NRM was measured and gradually removed and replaced by a new thermal magnetization. This was achieved by heating the samples alternatively in zero ($Z$) and a 60 μT applied ($A$) field in a Magnetic Measurements MMTD-80 thermal demagnetizer. Besides the conventional $Z/A$ steps, pTRM

and pTRM tail checks (Riisager and Riisager, 2001) were performed to ensure the absence of alteration and multidomain behavior within the magnetic remanence carriers, the remanent magnetization measurements were also performed on a 2G Enterprises superconducting rock magnetometer. Results were represented as Arai plots where NRM lost is plotted against the TRM gained (both normalized to the initial NRM), along with the pTRM and tail checks (Yu and Dunlop, 2003). Additionally Zijderveld diagrams were also plotted using the steps performed in zero field to check the directional uniformity of the NRM vector. For each site every sample-datum was plotted as a Gaussian function and, to compute an overall archaeointensity value, a function (usually a Gaussian too) was fitted to the sum of all individual results. Samples with no linear Arai plots (Chauvin et al., 2005), negative pTRM checks or $f$ values lower than 0.5 (Biggin and Thomas, 2003) were not used to get the overall intensity estimate. Positive pTRM checks were defined as those with a difference between the original pTRM and the pTRM check lower than 10 percent of the total TRM acquired (Chauvin et al., 2000).

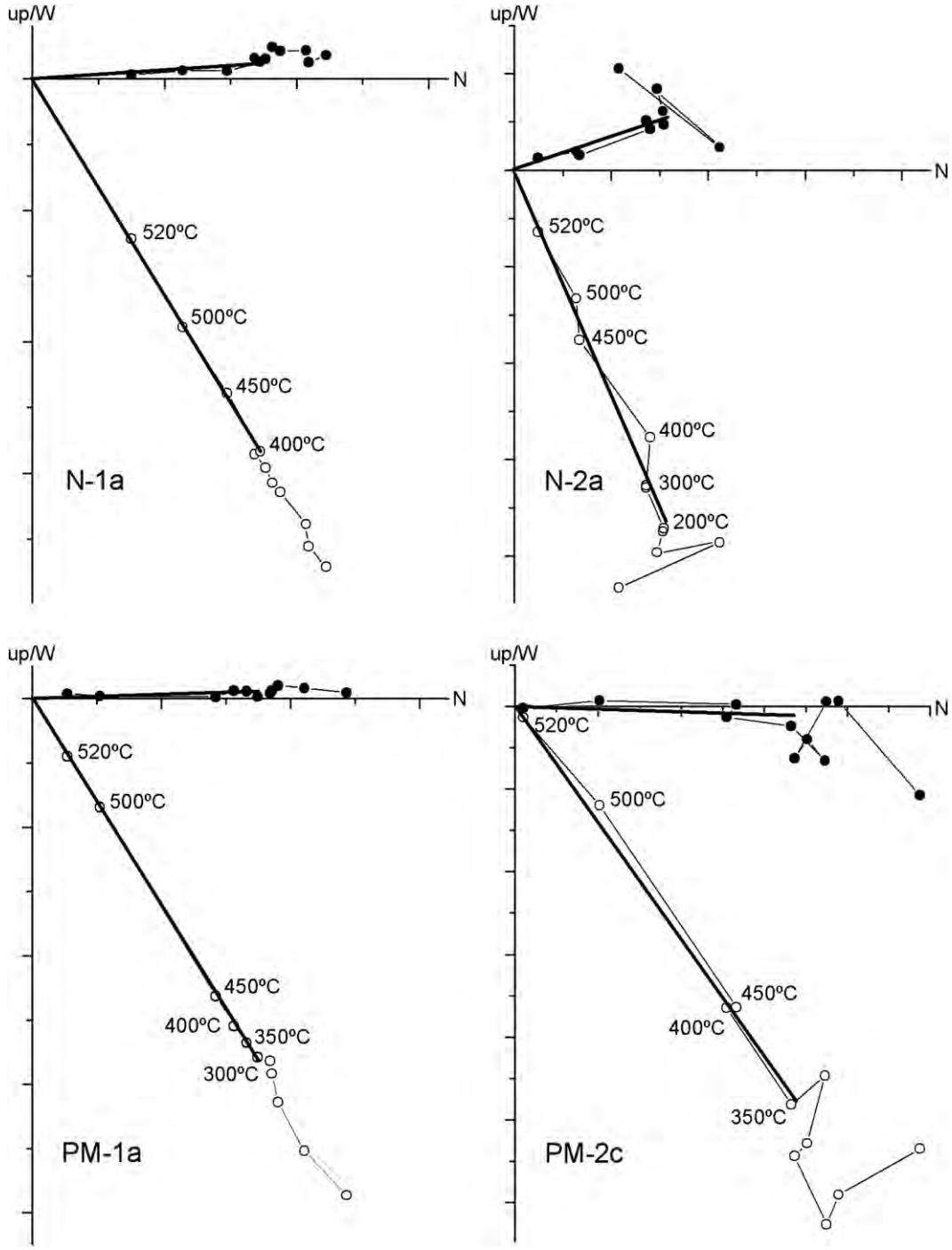


**Fig. 3.** Representative Zijderveld plots depicting the orthogonal projection of the remanent magnetization vectors during progressive demagnetization for different specimens from (top) Neapolis and (bottom) Pheradi Majus. Open (solid) symbols represent projections on vertical (horizontal) planes. Lines indicate the ChRM directions.

## 5. Results and discussion

### 5.1. Archaeodirectional results and discussion

Representative Zijderveld diagrams of specimens from Neapolis and Pheradi Majus are shown in Fig. 3. When two specimens were available from an independently oriented sample (i.e. a single core), either a mean sample direction was calculated (if both show similar MAD values) or the most reliable demagnetization experiment was adopted as the value for the particular sample (Gómez-Paccard and Beamud, 2008). A total of 52 specimens were analyzed (12 from N-1, 9 from N-2, 24 from PM-1 and 7 from PM-2). The rate of successful measurements has been 100% for samples from Neapolis, whereas 8 specimens were rejected from PM-1 and 3 from PM-2 due to MAD values higher than 5 (4), Zijderveld plots not pointing to the origin (4) or low demagnetization rate (3). Fig. 4 shows the stereographic projection of the non-rejected archaeomagnetic directions calculated for each sample, together with mean direction and $\alpha_{95}$ error circles for each structure. From Fig. 4 and Table 2 it is apparent that mean direction for the 2 kilns from Neapolis (N-1 and N-2) are distinctly different whereas the two kilns from Pheradi Majus (PM-1 and PM-2) are statistically indistinguishable. For this reason, results from PM-1 and PM-2 were merged to get a mean direction for the site.

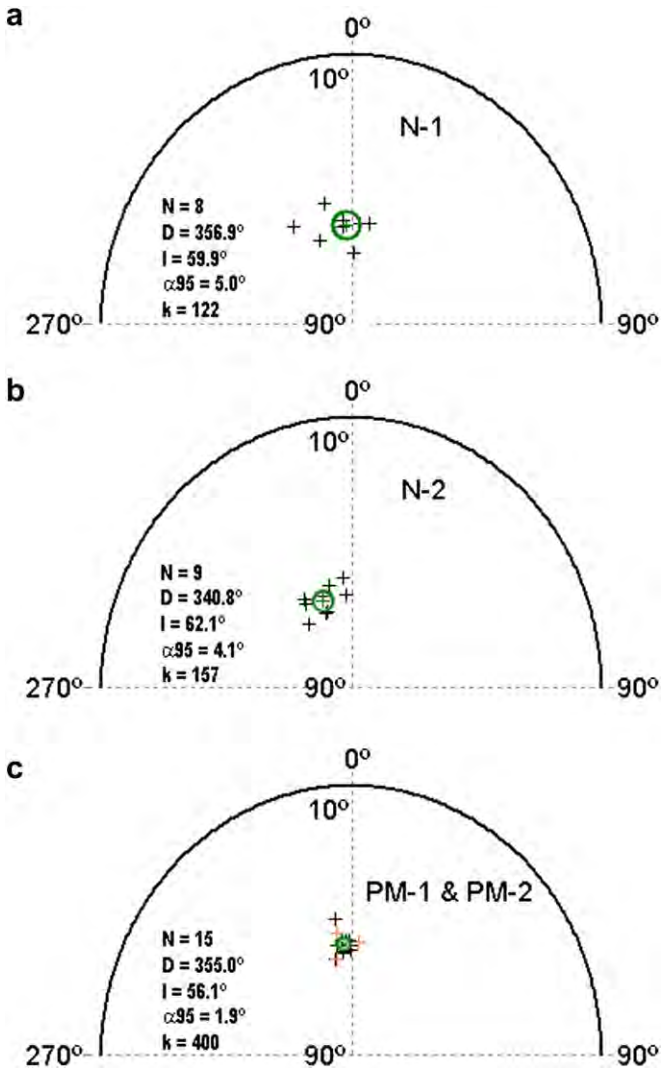


**Fig. 4.** Stereographic projection of the archaeomagnetic directions calculated for each sample, together with the mean direction and $\alpha_{95}$ error circles for (a) N-1 kiln, (b) N-2 kiln (both from Neapolis) and (c) PM-1 and PM-2 kilns from Pheradi Majus. *N* indicates the number of independently oriented samples taken into account for the calculation of the mean; *D* and *I* stands for Declination and Inclination; $\alpha_{95}$ and *k*, 95% confidence cone of mean directions and precision parameter from Fisher statistics.

**Table 2**
Archaeomagnetic directional results.

| Name | Lat (°N) | Long (°E) | *n*/*N* | *D* (°) | *I* (°) | *k* | $\alpha_{95}$ (°) |
|---|---|---|---|---|---|---|---|
| Neapolis (N-1) | 36.44 | 10.72 | 12/8 | 356.9° | 59.9° | 121.9 | 5.0 |
| Neapolis (N-2) | 36.44 | 10.72 | 9/9 | 340.8° | 62.1° | 157.0 | 4.1 |
| Pheradi Majus (PM-1) | 36.25 | 10.40 | 16/12 | 354.8° | 56.0° | 440.0 | 2.1 |
| Pheradi Majus (PM-2) | 36.25 | 10.40 | 4/3 | 355.8° | 56.4° | 230.5 | 8.7 |
| Pheradi Majus (merged) | 36.25 | 10.40 | 20/15 | 355.0° | 56.1° | 400.1 | 1.9 |

Columns from left to right: Name, name of the site (structure); Lat. and Long., Latitude and Longitude of the site; *n*/*N*, number of specimens analyzed (*n*)/independently oriented samples taken into account in the calculation of the mean site direction (*N*); *k* and $\alpha_{95}$, precision parameter and 95% confidence limit of characteristic remanent magnetisation, from Fisher statistics.

Comparing the results with the SCHA.DIF.3K and CALS3K.3 models we obtained probability density functions of possible dates for both declination and inclination. The intersection of these functions produces the most probable dates according to each model (see Figs. 5 and 6, and Table 3).

The two kilns sampled at Neapolis produce different results. For the N-1 structure, using SCHA.DIF.3K model, the combined probability function indicates basically two solutions (AD 440–699 or AD 1607–1731). The first interval is in agreement with archaeological evidence (6th–7th century AD) and therefore the interval AD 1607–1731 is not plausible. For the N-2 structure, again using SCHA.DIF.3K, we get a narrow distribution probability function pointing to the 18th century against all archaeological evidence. In fact, archaeological evidence indicates that N-1 and N-2 structures should be contemporary. Samples drilled on N-2 structure come from the only currently accessible part of the kiln, which is the top of a cylindrical wall made of thin rectangular blocks of a sort of conglomerate (see Fig. 2). Some of these blocks (not sampled) were actually loose and it is possible that the whole ensemble had been displaced during the excavations. Re-sampling of N-2 structure at a lower level, when possible, could confirm this hypothesis. For the moment, we can only rely on N-1 results to date the kilns from the south-west part of the *Nympharum domus* in Neapolis. Probability distributions using the CALS3K.3 model are similar though broader (see Table 3).

The results for the kilns sampled at Pheradi Majus show only one solution (Fig. 5c), using SCHA.DIF.3K this solution is the time interval AD 430–516. Actually, using the entire temporal range of application of the model, another peak emerges around year 0, which can be rejected according the archaeological evidence, that points to 4th and 5th centuries. Therefore, the dating obtained from combining archaeomagnetism and archaeological evidence indicates the 5th century as the most probable age of the last use of the kilns in the artisan's neighborhood from Pheradi Majus. Using CALS3K.3 the distribution probability functions are similar but again broader, here to such an extent that probability peaks centered around 0 and 423 almost overlap (Fig. 6c).

It is worth to mention that the presented date intervals are the solutions to a given mathematical approach, but do not imply annual precision in the dating method. Taken into account the maxima from the obtained probability distribution functions using either SCHA.DIF.3K or CALS3K.3 models, the last use of kilns from Neapolis and Pheradi Majus appear to be almost contemporary, being that of Pheradi Majus slightly older.

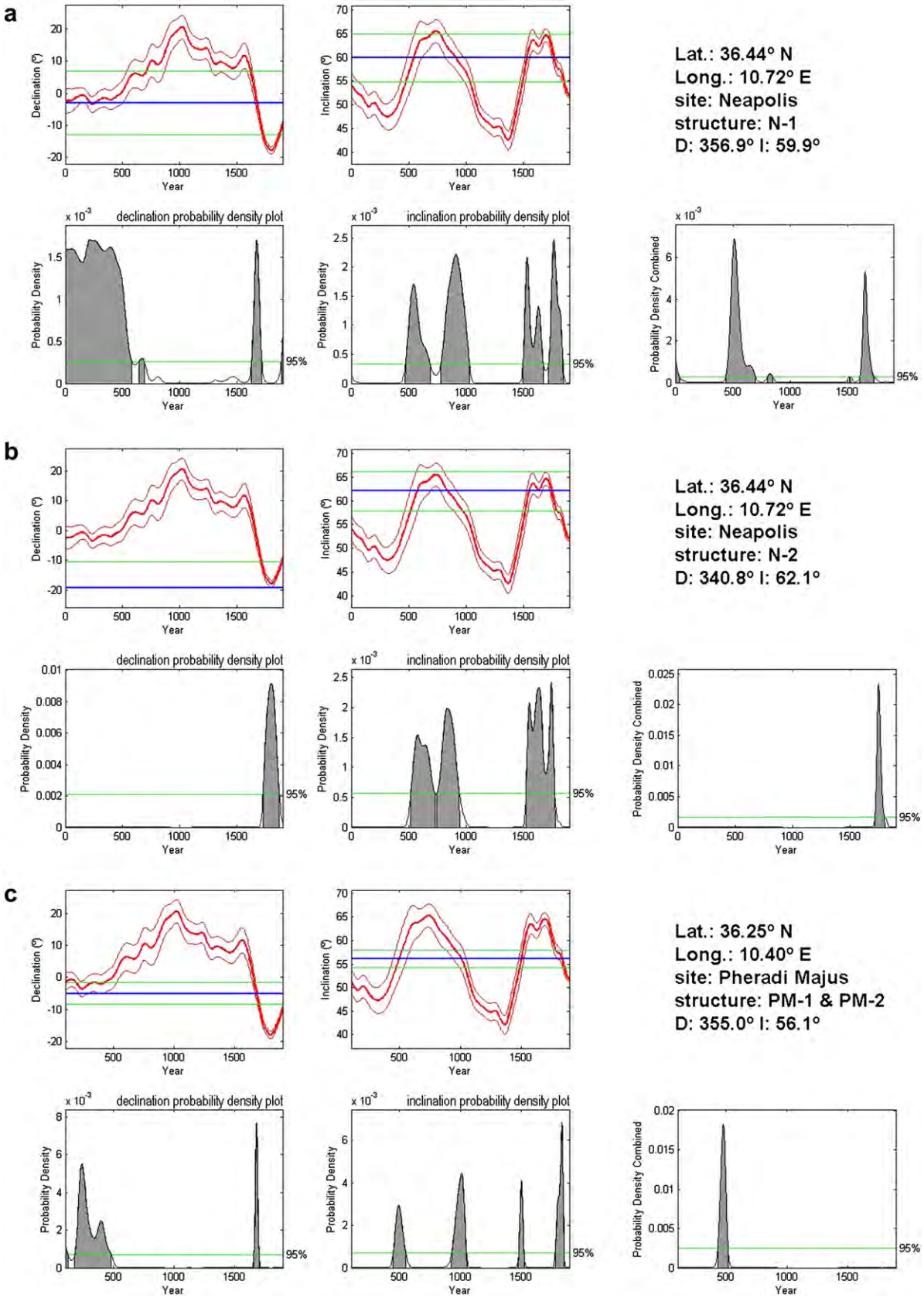


**Fig. 5.** Probability-of-age density functions obtained with the Matlab tool from Pavón-Carrasco et al. (2011) for (a) N-1 kiln, (b) N-2 kiln (both from Neapolis) and (c) PM-1 and PM-2 kilns from Pheradi Majus, using SCHA.DIF.3K model. On the right: location of the sites, experimental mean directions and combined (declination and inclination) probability functions.

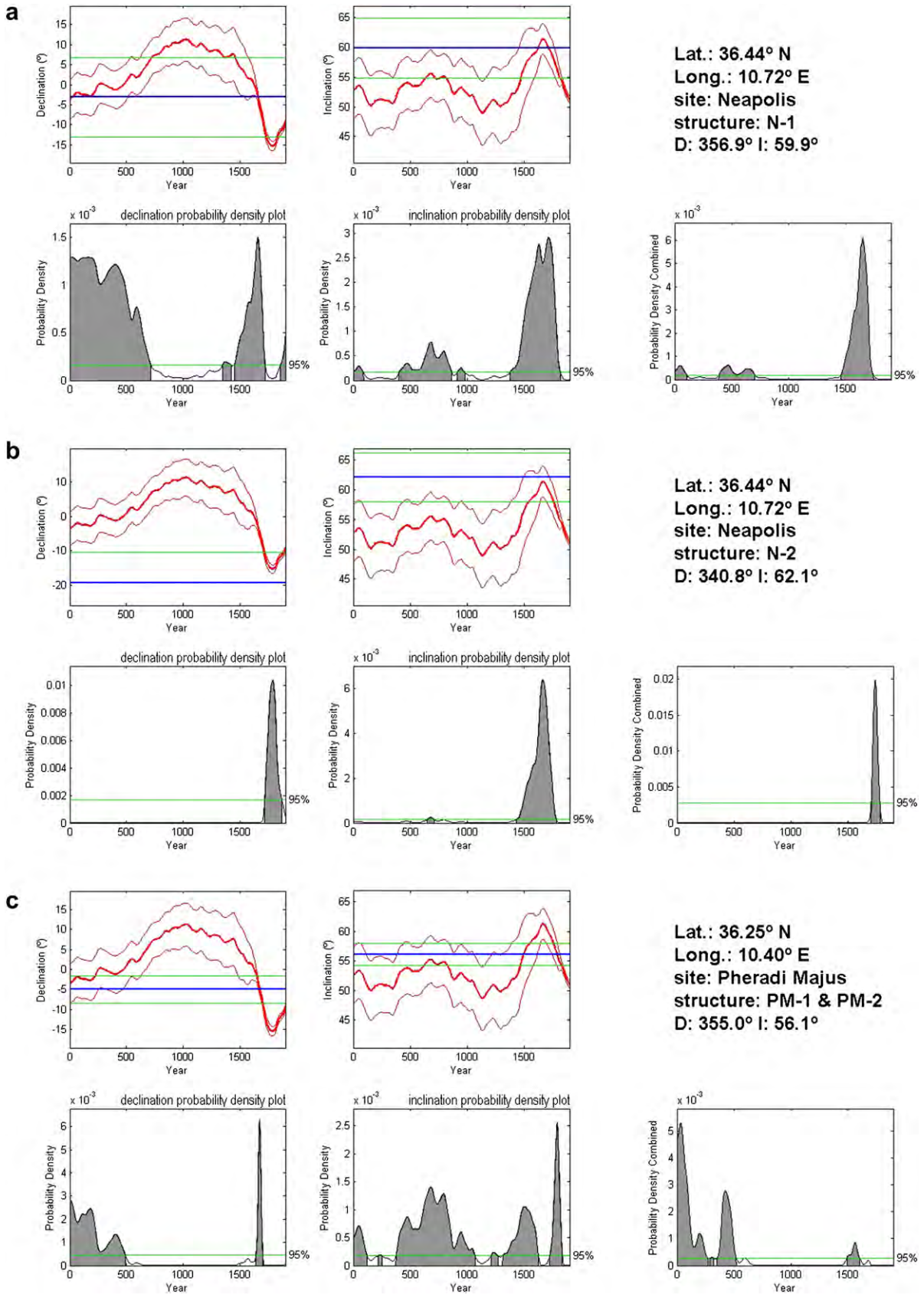


**Fig. 6.** Probability-of-age density functions obtained with the Matlab tool from Pavón-Carrasco et al. (2011) for (a) N-1 kiln, (b) N-2 kiln (both from Neapolis) and (c) PM-1 and PM-2 kilns from Pheradi Majus, using CALS3K.3 model. On the right: location of the sites, experimental mean directions and combined (declination and inclination) probability functions.

**Table 3**
Archaeomagnetic ages using SCHA.DIF.3K and CALS3K.3 geomagnetic models for kilns from Neapolis (N-1 and N-2) and Pheradi Majus (PM). Main solutions and maxima refer to the obtained probability time-distributions which are characterized by well-defined peaks and only in some cases secondary low-probability features.

| Structure | Model | Main solutions | Maxima[a] | Presumed archaeological age |
|---|---|---|---|---|
| N-1 | SCHA.DIF.3K | AD 440–699 | 515 | 6th–7th AD |
| | | AD 1607–1731 | 1654 | |
| N-1 | CALS3K.3 | AD 389–706 | 464 | 6th–7th AD |
| | | AD 1461–1747 | 1649 | |
| N-2 | SCHA.DIF.3K | AD 1717–1802 | 1750 | 6th–7th AD |
| N-2 | CALS3K.3 | AD 1739–1837 | 1791 | 6th–7th AD |
| PM | SCHA.DIF.3K | AD 430–516 | 477 | 4th–5th AD |
| PM | CALS3K.3 | AD 0–273 | 33 | 4th–5th AD |
| | | AD 353–520 | 423 | |

[a] Maxima correspond to the best fits between the archaeomagnetic data and the models but do not necessarily imply the best true age of the feature.

### 5.2. Archaeointensity results and discussion

Representative Arai plots of specimens from Pheradi Majus, Leptiminus and Sullecthum are shown in Fig. 7. A total of 47 specimens were analyzed (12 from PM-SS, 23 from L-SS and 12 from S-SS), all of them exhibit linear Arai plots. From these, only 10 were rejected (4 from Pheradi Majus, 2 from Leptiminus and 4 from Sullecthum) due to low $f$ values (6) or negative pTRM checks (4). Although the Arai plots show a high degree of alignment, the uncertainties associated to each archaeointensity determination are quite large. This is due to a significant viscous component in the remanence that produces large differences between the original NRM and the NRM remaining after demagnetized only up to 100 °C.

Fig. 8 shows plots of the sum of all accepted individual archaeointensity results per site and the fittings to obtain overall archaeointensity estimates for each site. The sum of results from Pheradi Majus produces a bimodal distribution that can be fitted with two Gaussians: the main component equals 88% of the area

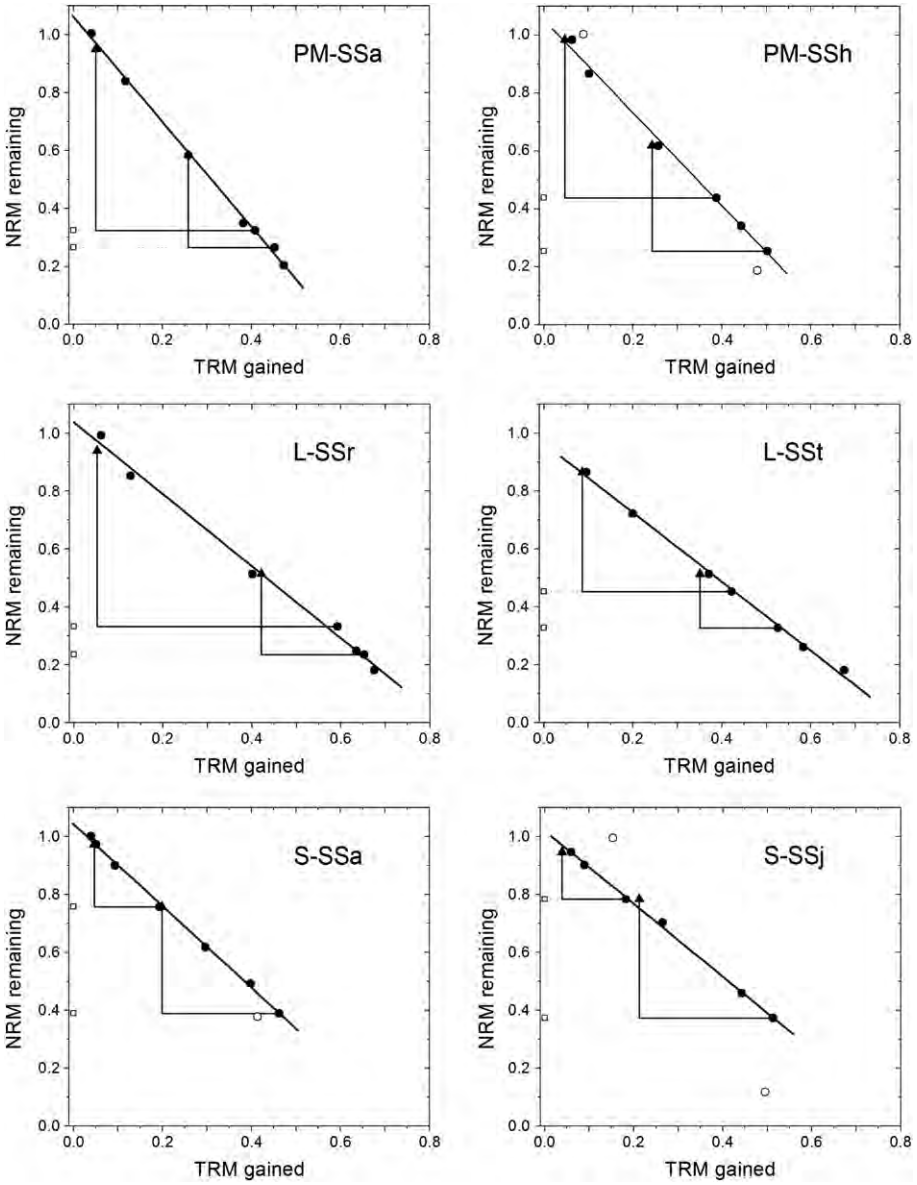


**Fig. 7.** Representative plots of normalized NRM remaining against TRM gained for specimens from Pheradi Majus (PM-SS), Leptiminus (L-SS) and Sullecthum (S-SS).

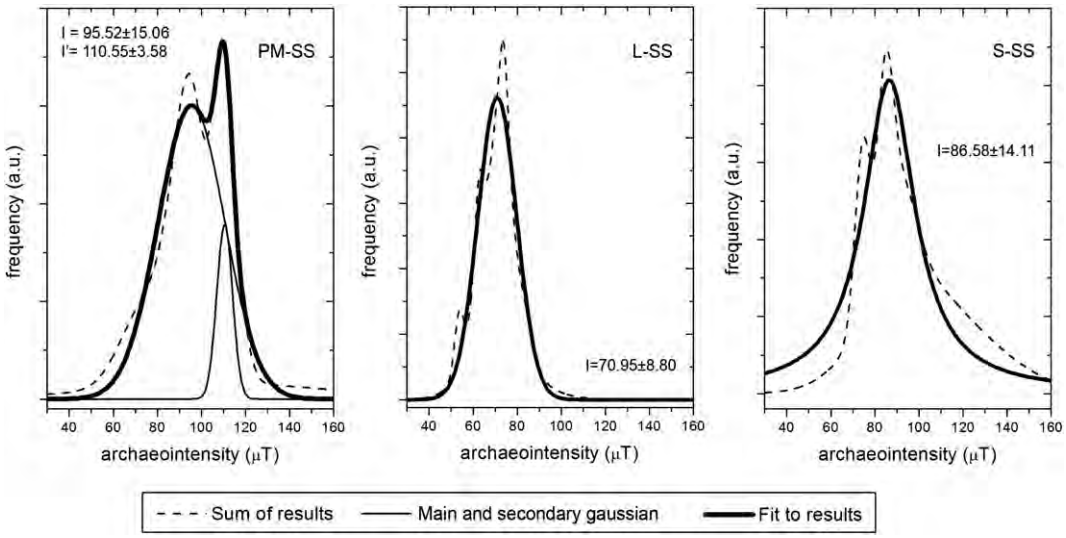


**Fig. 8.** Computation of mean archaeointensities for sites: (left) Pheradi Majus, (middle) Leptiminus and (right) Sullecthum. Dashed line is the sum of all accepted individual archaeointensity results for the site and solid line is the fitting to those sums.

and is a wide peak centered at 95.52 μT, the secondary peak is much smaller and centered at an unreasonably high value of 110.55 μT. The presence of this secondary peak is basically due to 2 specimens that yielded high quality results but with unusually high archaeointensities, we can assume that the representative intensity for the site is the one from the main peak. The sum of results from Leptiminus and Sullecthum show single-peak distributions that have been fitted by a Gaussian and a Lorentzian function respectively to obtain the archaeointensity estimates (70.95 μT for Leptiminus and 86.58 μT for Sullecthum). The Lorentzian function was chosen for Sullecthum due to the longer tail-ends of its distribution of results. The width of the fitted functions is important for the three estimates and results in quite large uncertainties. The overall archaeointensity estimates are thus 95.52 ± 15.06 μT, 70.95 ± 8.80 μT and 86.58 ± 14.11 μT for Pheradi Majus, Leptiminus and Sullecthum sites respectively.

Comparing the results with the SCHA.DIF.3K and CALS3K.3 models it is apparent that the three archaeointensity estimates are much higher than the model predictions for the time interval indicated by archaeological evidence (see Fig. 9). Indeed, the SCHA.DIF.3K predicts geomagnetic field intensity values with small fluctuations around a mean of only 50 μT for the first five centuries AD. Higher values are only predicted later, during the 9th century, but even so, they reach a maximum value of only 70 μT. Concerning CALS3K.3 the fluctuations are smoother, with a mean value a bit higher for the first five centuries (~55 μT) but a lower maximum during the 9th century (~65 μT).

Within the available archaeomagnetic datasets, archaeointensities higher than 70 μT are rare and even rarer at medium-low latitudes. However, there are not known restrictions regarding the maximum field strength of the geomagnetic field or its maximum rate of change (Erez Ben-Yosef et al., 2009). Exceptional high-archaeointensity values up to 130 μT have been reported for samples in southern Jordan (latitude 30.7° N) during the 10th century BC (Erez Ben-Yosef et al., 2009). Within the time interval we are interested in, some high archaeointensities can also be found and closer to Tunisia. Values ranging from 75 μT to 92 μT from Viterbo, Italy (latitude 42.6° N) in the 6th–7th century AD, are included in the Cals3k3 dataset (Donadini et al., 2009), where a value of 92.5 μT is also reported for this location for the year 420 ± 50 AD.

A direct consequence of the rarity of archaeointensity values above 75 μT is that archaeomagnetic field models do not predict high arqueointensities. Despite the large uncertainties associated to the measured archaeointensities from Roman sites in Tunisia, it is clear that the experimental data point to higher values than those predicted by the models. It is well-known that the reliability of the model predictions is largely dependent on the availability of experimental data near the area and time under study (Casas et al., 2008). Within the Cals3k3 dataset there are not archaeointensities attributed to one of the first 700 years AD from Tunisia, there are only data from two locations in the neighboring Libya: a set of 12 values (one or two per century) near the southern border of Tunisia (latitude 30.9° N) with values ranging from 38.4 μT to 53.5 μT and a single value from Tripoli (latitude 32.8° N) with 55 μT for the year 125 ± 25 AD. The first location is more than 500 km south from the sites studied here and the second is nearly 400 km south-east from they. The closest European data to our Tunisian sites are from Italy, to the north-east: Lipari, at nearly 500 km (bearing a single archaeointensity value of 52.4 μT from the year 543 ± 25 AD) and Naples and Sybaris, at more than 600 km (with three

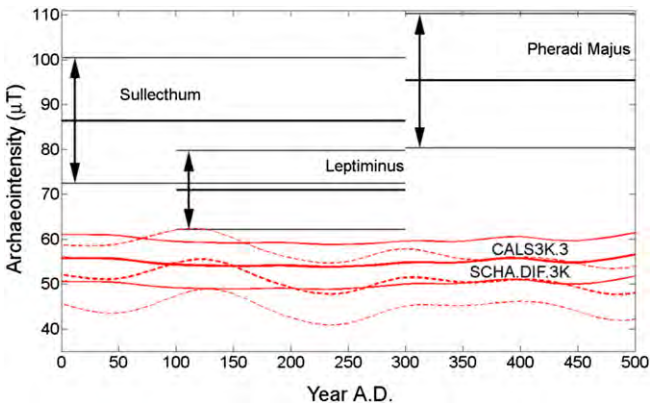


**Fig. 9.** Comparison between the archaeomagnetic-field intensity variations predicted by CALS3K.3 (solid line) and SCHA.DIF.3K (dashed line) models for the first 500 years AD in the studied area and the experimentally obtained values with indication of their presumed archaeological ages. Indication of intensity uncertainty is given for all data (95% confidence level).

archaeointensities from the 1st century AD with values of 61.2, 71.34 and 75.3 μT). Taken into account the scarce and distant data it is not surprising that predictions of models based on these data and actual experimental data do not fit.

Regarding Tunisian data from other time intervals (besides the first 700 years AD) the outlook does not change, data is really scarce. Paradoxically, data from Carthage appear in the pioneering paper from Thellier and Thellier (1959). This old data comprises two intensities (77 μT and 71 μT) included in Cals3k3 dataset attributed to years 600 BC and 146 BC respectively. Recently, Del Vigo and McIntosh (2010) have published data from five kilns near Kairouan (less than 100 km from our studied sites) with intensities around 67 μT and 60–65 μT for the 9th and the 11th centuries AD. The ages of these four kilns as well as the materials studied in the present paper should be more constrained in order to describe more accurately the evolution of the geomagnetic strength for the Tunisian area. This could be done using archaeodirections, since the existing models seem to be consistent with the experimental data and therefore, dating is possible using directional data.

## 6. Conclusions

The ages of last use of the kilns in Neapolis and Pheradi Majus have been constrained using archaeomagnetic directional data. Comparing experimental data with the SCHA.DIF.3K and CALS3K.3 models emerges that N-1 kiln (in Neapolis) was probably active until the early 6th century, whereas PM-1 and PM-2 kilns (in Pheradi Majus) were active until the middle 5th century. On the studied area, the mentioned models behave as proficient tools to date archaeological sites when using directional data.

In contrast, these models fail to predict the experimental archaeointensities from the three studied sites and hence its applicability seems to be limited. The archaeointensities produced in the present investigation have relatively large uncertainties thought the single measurements have been filtered using strict selections criteria. Sampling at the sites could be improved in the future and extended to Neapolis if excavation campaigns are undertaken. Despite present uncertainties, data point to a higher than predicted geomagnetic field strength for the first centuries AD in the studied area. This unattended result should be object of further investigation.

New archaeomagnetic studies in areas with few or no previous collected data are necessary to act as a feedback to improve the resolution and applicability of geomagnetic field models. However, the new data should be accompanied with a precise age determined independently. Specifically, in the case of archaeointensity databases and models, even though it would be preferable to use age ranges determined by non-magnetic methods, archaeodirectional ages could, to some extend, constraint age ranges and thus, contribute to the feedback.

Tunisia is a country with a very rich archaeological heritage and thus with a huge potential to apply archaeomagnetic techniques. Combined archaeodirection and archaeointensity studies similar to the one undertaken in Pheradi Majus should be extended, when possible, to other Tunisian and North African sites. The archaeomagnetic techniques provide an important new dating resource for archaeologists working in northern Africa.

## Acknowledgments

We are grateful to Mounir Fantar, Néjib Ben Lazreg, Samir Ouanallah and Slim Ben Cherifia, researchers at the Tunisian Institut National du Patrimoine, to allow access and sampling into the archaeological sites. We thank Siwar Baklouti and Marta Moreno for their support during field work. We also would like to acknowledge two anonymous reviewers for their helpful and insightful comments. This research was funded by the Spanish Ministerio de Ciencia y Innovación (project HAR2010-16953) and the Agencia Española de Cooperación Internacional para el Desarrollo (Spain-Tunisia bilateral project A1/039844/11).

## References

Ben Moussa, M., 2007. La production de sigillées africaines. Recherches d'histoire et d'archeologie en Tunisie septentrionale et centrale. Ed. Universitat de Barcelona, Barcelona, 306 pp.

Ben-Yosef, E., Tauxe, L., Levy, T.E., Shaar, R., Ron, H., Najjar, M., 2009. Geomagnetic intensity spike recorded in high resolution slag deposit in Southern Jordan. Earth Planet. Sci. Lett. 287, 529–539.

Biggin, A.J., Thomas, D.N., 2003. The application of acceptance criteria to results of Thellier palaeointensity experiments performed on samples with pseudo-single-domain-like characteristics. Phys. Earth Planet. Inter. 138, 279–287.

Casas, Ll., Briansó, J.L., Álvarez, A., Benzzi, K., Shaw, J., 2008. Archaeomagnetic intensity data from the Saadien Tombs (Marrakech, Morocco), late 16th century. Phys. Chem. Earth 33, 474–480.

Casas, Ll, Incoronato, A., 2007. Distribution analysis of errors due to relocation of geomagnetic data using the Conversion via Pole' (CVP) method: implications on archaeomagnetic data. Geophys. J. Int. 169, 448–454.

Chauvin, A., Garcia, Y., Lanos, Ph., Laubenheimer, F., 2000. Palaeointensity of the geomagnetic field recovered on archaeomagnetic sites from France. Phys. Earth Planet. Inter. 120, 111–136.

Chauvin, A., Roperch, P., Levi, S., 2005. Reliability of geomagnetic palaeointensity data: the effects of the NRM fraction and concave-up behaviour on palaeointensity determinations by the Thellier method. Phys. Earth Planet. Inter. 150, 265–286.

Coe, R.S., 1967. Paleointensities of the Earth's magnetic field determined from Tertiary and Quaternary rocks. J. Geophys. Res. 72, 3247–3262.

Darmon, J.P., 1980. Nympharum domus, les pavements de la maison des nymphes à Néapolis (Nabeul, Tunisie) et leur lecture. Brill Ed., Leiden, 270 pp.

Del Vigo, A., McIntosh, G., 2010. Testing the multispecimen palaeointensity technique on archaeological material: preliminary results from Tunisian baked clays. Física de la Tierra 22, 163–174.

Donadini, F., Korte, M., Constable, C.G., 2009. Geomagnetic field for 0–3 ka: 1. New data sets for global modeling. Geochem. Geophys. Geosyst. 10, Q06007.

Fisher, R.A., 1953. Dispersion on a sphere. Proc. Roy. Soc. London A 217 (1130), 295–305.

Gibbins, D., 2001. A Roman shipwreck of c. AD 200 at Plemmirio, Sicily: evidence for North African amphora production during the Severan Period. World Archaeol. 32 (3), 311–334.

Gómez-Paccard, M., Beamud, E., 2008. Recent achievements in archaeomagnetic dating in the Iberian Peninsula: application to Roman and Medieval Spanish structures. J. Arch. Sci. 35, 1389–1398.

Gómez-Paccard, M., Chauvin, Lanos, Ph., McIntosh, G., Osete, M.L., Catanzariti, G., Ruiz-Martínez, V.C., Núñez, J.I., 2006. First archaeomagnetic secular variation curve for the Iberian Peninsula: comparison with other data from western Europe and with global geomagnetic field models. Geochem. Geophys. Geosyst. 7, Q12001. doi:10.1029/2006GC001476.

Hervé, G., Schnepp, E., Chauvin, A., Lanos, Ph., Nowaczyk, N., 2011. Archaeomagnetic results on three Early Iron Age salt-kilns from Moyenvic (France). Geophys. J. Int.. doi:10.1111/j.1365-246X.2011.04933.x.

Keenleyside, A., Schwarcz, H., Stirling, L., Ben Lazreg, N., 2009. Stable isotopic evidence for diet in a Roman and Late Roman population from Leptiminus, Tunisia. J. Arch. Sci. 36 (1), 51–63.

Kirschvink, J.L., 1980. The least-squares line and plane and the analysis of paleomagnetic data. Geophys. J. Int. 62 (3), 699–718.

Korte, M., Donadini, F., Constable, C.G., 2009. The geomagnetic field for 0-3 ka, Part II: A new series of time-varying global models. Geochem. Geophys. Geosyst. 10, Q06008. doi:10.1029/2008GC002297.

Le Goff, M., Gallet, Y., Genevey, A., Warmé, N., 2002. On archeomagnetic secular variation curves and archeomagnetic dating. Phys. Earth Planet. Inter. 134 (3–4), 203–211.

Lengyel, S.N., Eighmy, J.L., Van Buren, M., 2011. Archaeomagnetic research in the Andean highlands. J. Arch. Sci. 38, 147–155.

Leone, A., 2007. Changing Townscapes in North Africa from Late Antiquity to Arab Conquest. Edipuglia, Bari, 357 pp.

Mattingly, D.J., Stone, D., Stirling, L., Ben Lazreg, N., 2000. In: Mattingly, D.J., Salmon, J. (Eds.), Economies Beyond Agriculture in the Classical World. Routledge Press, London, pp. 66–89.

Nacef, J., 2007. In: Mrabet, A., Remesal Rodriguez, J. (Eds.), Africa et in Hispania: Etudes sur l'huile africaine. Universitat de Barcelona, Barcelona, pp. 41–54.

Nacef, J., 2008. Production de la céramique antique et ateliers dans la région de Salakta et Ksour Essef. Université de Tunis: Faculté des Sciences Humaines et Sociales (doctoral thesis).

Pavón-Carrasco, F.J., Osete, M.L., Torta, J.M., Gaya-Piqué, L.R., 2009. A regional archaeomagnetic model for Europe for the last 3000 years, SCHA.DIF.3K: applications to archaeomagnetic dating. Geochem. Geophys. Geosyst. 10, Q03013. doi:10.1029/2008GC002244.

Pavón-Carrasco, F.J., Rodríguez-González, J., Osete, M.L., Torta, J.M., 2011. A matlab tool for archaeomagnetic dating. J. Arch. Sci. 38 (2), 408–419.
Peacock, D.P.S., Bejaoui, F., Belazrec, N., 1989. Roman Amphora Production in the Sahel Region of Tunisia. École Française de Rome, Rome, 1–2 pp. (Publications de l'École française de Rome, 114).
Riisager, P., Riisager, J., 2001. Detecting multidomain grains in Thellier palaeomagnetic experiments. Phys. Earth Planet. Inter. 125, 111–117.
Sherriff, B.L., Court, P., Johnston, S., Stirling, L., 2002a. The source of raw materials for Roman pottery from Leptiminus, Tunisia. Geoarchaeology 17 (8), 835–861.
Sherriff, B.L., McCammon, C., Stirling, L., 2002b. A Mössbauer study of the color of Roman pottery from the Leptiminus archaeological site, Tunisia. Geoarchaeology 17 (8), 863–874.
Sternberg, M., 2000. Données sur les produits fabriqués fans une officine de Neapolis (Nabeul, Tunisie). Mélanges de l'Ecole française de Rome. Antiquité 2 (1), 135–153.
Stirling, L., Stone, D., Ben Lazreg, N., 2000. Roman kilns and rural settlement: interim report of the 1999 season of the Leptiminus Archaeological Project. Echos du Monde Classique/Classical Views 44 (19), 170–224.
Stirling, L.M., Mattingly, D.J., Ben Lazreg, N. (Eds.), 2001. Leptiminus (Lamta): A Roman Port City in Tunisia. Report 2: The East Baths, Cemeteries, Kilns, Venus Mosaic, Site Museum, and Other Studies. (Journal of Roman Archaeology supplement 41), Portsmouth, Rhode Island.
Thellier, E., Thellier, O., 1959. Sur l'intensité du champ magnétique terrestre dans le passé historique et géologique. Ann. Géophysique 15, 285–376.
Whittaker, C.R., 2000. In: Bowman, A.K., Garnsey, P., Rathbone, D. (Eds.), The Cambridge Ancient History: The High Empire, A.D. 70–192. Cambridge University Press, Cambridge, pp. 514–546.
Yu, Y., Dunlop, D.J., 2003. On partial thermoremanent magnetization tail checks in Thellier paleointensity determination. J. Geophys. Res. 108. doi:10.1029/2003JB002420.
Zananiri, I., Batt, C.M., Lanos, Ph., Tarling, D.H., Linford, P., 2007. Archaeomagnetic secular variation in the UK during the past 4000 years and its application to archaeomagnetic dating. Phys. Earth Planet. Inter. 160 (2), 97–107.
Zijderveld, J.D.A., 1967. AC Demagnetization of rocks: analysis of results. In: Collison, D.W., Creer, K.M., Runcorrn, S.K. (Eds.), Methods in Paleomagnetism. Elsevier, New York, pp. 254–286.